Journal of Thermal Analysis and Calorimetry, Vol. 89 (2007) 2, 643–647

LOW-TEMPERATURE HEAT CAPACITY AND THERMODYNAMIC PROPERTIES OF CRYSTALLINE LEAD FORMATE

J. Zhang[1,2], *Y. Y. Liu*[1,2], *Z. H. Zhang*[1,2], *X. C. Lv*[1,2], *L. X. Sun*[1*], *F. Xu*[1], *Z. C. Tan*[1], *T. Zhang*[1] *and Y. Sawada*[3]

[1]Materials and Thermochemistry Laboratory, Dalian Institute of Chemical Physics, Chinese Academy of Sciences, Dalian 116023, P.R. China
[2]Graduate School of the Chinese Academy of Sciences, Beijing 100049, P.R. China
[3]Department of Nanochemistry, Faculty of Engineering, Tokyo Polytechnic University, 1583 Iiyama, Atsugi, Kanagawa 243-0297, Japan

As one 3-D coordination polymer, lead formate was synthesized; calorimetric study and thermal analysis for this compound were performed. The low-temperature heat capacity of lead formate was measured by a precise automated adiabatic calorimeter over the temperature range from 80 to 380 K. No thermal anomaly or phase transition was observed in this temperature range. A four-step sequential thermal decomposition mechanism for the lead formate was found through the DSC and TG-DTG techniques at the temperature range from 500 to 635 K.

Keywords: *adiabatic calorimetry, coordination polymers, DSC, heat capacity, lead formate, phase transition, TG-DTG*

Introduction

The construction of infinite frameworks by linking metal ions with small organic multifunctional ligands is an attractive topic on the interface between chemistry and materials science. The most promising applications of coordination polymers may include magnetic exchange, non-linear optical (NLO), catalysis, or hydrogen storage [1, 2].

Lead formate [$Pb(HCOO)_2$; CA registry No. 811-54-1] with simple component, comprises a 3-D polymeric network [3, 4], which has been referred to as a new material in the field of non-linear optical applications [5]. Some thermal behaviors of lead formate have been already investigated by a number of researchers [6, 7]. To our best knowledge, there has been no report on molar heat capacity of lead formate in literature. Heat capacities determinations of various compounds have attracted many researchers' attention [8–11]. For the application of the compound, thermodynamic properties of this substance are urgently required.

In the present work, the low-temperature heat capacity of lead formate has been measured over the temperature range from 80 to 380 K. The thermal decomposition characteristics of this compound were investigated by differential scanning calorimetry (DSC) and thermogravimetric analysis (TG-DTG).

Experimental

Sample preparation

All materials were commercially available and were of analytical grade unless stated elsewhere. Lead nitrate (3.3 g, 10.0 mmol) was dissolved in DMF/1, 4-dioxane (2:1 by volume, 360 mL). The mixture was stirred at room temperature until lead nitrate entirely dissolved. Then, formic acid (920 mg, 755 μL, 20.0 mmol) was slowly added to the above transparent mixed solution. Then, the solution was distributed to twenty vials of 20 mL. The vials were open, and the solvent was slowly volatilized. After four weeks, polyhedral crystals were produced, collected, and washed three times with DMF (50 mL).

Elemental analyses for $C_2H_2O_4Pb$ found (%): C, 7.78; H, 0.43; calc. (%): C, 8.08; H, 0.68; FTIR (KBr pellet, 4000–400 cm^{-1}): 1629 and 1562 (OCO, str., asym.), 1352 (OCO, deform., asym.), 1338s (OCO, str., sym.), 778 and 764 (OCO, deform., sym.). The content of lead was determined by atomic absorption spectrometer.

The crystal structure of lead formate was determined by the single crystal X-ray diffraction. Crystal data: $C_2H_2O_4Pb$, orthorhombic, $P2_12_12_1$, a=6.4934(6) Å, b=7.4232(7) Å, c=8.7240(8) Å, V=420.51(7) $Å^3$, Z=4. The values are in excellent agreement with earlier published values [4].

* Author for correspondence: lxsun@dicp.ac.cn

1388–6150/$20.00

Akadémiai Kiadó, Budapest, Hungary
Springer, Dordrecht, The Netherlands

All chemical and elemental analyses showed that the purity of the sample prepared was enough high to the heat capacity measurements.

Methods

Elemental analysis was carried on PE-2400 II Series CHNS/O analyzer. FTIR spectra was recorded on Bruker Equinox 55 infrared spectrometer using KBr pellet in the range of 4000–400 cm^{-1}. Atomic absorption spectra was performed by AA6650 Shimadzu atomic absorption spectrometer. The crystal data were collected with a Bruker Smart CCD area diffractometer equipped with graphite monochromated MoK_α radiation (λ=0.71073 Å) by the ω–2θ scan technique at 187(2) K.

Adiabatic calorimetry

The heat capacity measurements were carried out in a high-precision automated adiabatic calorimeter over the temperature range from 80 to 380 K. The calorimeter was established by Thermochemistry Laboratory of Dalian Institute of Chemical Physics, Chinese Academy of Sciences in PR China. The structure and principle of the calorimeter have been described in detail in the literature [12, 13]. Briefly, the automatic adiabatic calorimeter mainly consisted of a sample cell, a miniature platinum resistance thermometer, an electric heater, an adiabatic (or inner) shield, a guard (outer) shield, two sets of six-junctions chromel–copper (Ni: 55%, Cu: 45%) thermopiles installed between the calorimetric cell and the inner shield and between the inner and outer shields, respectively, and a high vacuum can. The evacuated chamber was kept within ca. 1 mbar during the heat capacity measurement so as to eliminate the heat loss owing to gas convection. Liquid nitrogen was used as the cooling medium.

Prior to the heat capacity measurement of the sample, the reliability of the calorimetric apparatus was verified by heat capacity measurements of the standard reference material-α-Al_2O_3 (NBS SRM-720). The results showed that the deviation of our calibration data from the recommended value of the former National Bureau of Standards [14] over the whole temperature range was within ±0.3%. The electrical energy introduced into the sample cell and the equilibrium temperature of the cell after the energy input were automatically collected by use of a Data Acquisition/Switch Unit (Model: 34970A, Agilent, USA) and processed by a computer on line.

The heat capacity measurements were continuously and automatically carried out by the standard procedure of intermittently heating the sample and alternately measuring the temperature. The heating duration was 10 min, and the temperature drift rates of the sample cell measured in an equilibrium period were generally within 10^{-3} to 10^{-4} K min^{-1} during the acquisition of all heat capacity data. The sample mass of lead formate used for heat capacity measurement was 13.9626 g, which was equivalent to 0.0470 mol, based on its molar mass of 297.24 g mol^{-1}.

Thermal analysis

DSC analysis was performed using a differential scanning calorimeter (Model: DSC 141, Setaram Co., France) with a heating rate of 10 K min^{-1}. Dry high purity nitrogen (99.999%) was used as a purge gas at a flow rate of 50 cm^3 min^{-1}. The mass of the sample used for DSC analysis was 9.0 mg. Two aluminum crucibles were used (capacity: 30 μL) and the reference crucible was empty. The calibrations for the temperature and heat flux of the calorimeter were performed before the determination of the sample. The temperature and heat flux were calibrated by measuring the melting points of Hg (99.99%), In (99.99%), Sn (99.99%), Pb (99.99%) and Zn (99.99%), at different heating rates.

A thermogravimetric analyzer (Model: Setsys 16/18, Setaram Co., France) was used for TG measurement of this sample under nitrogen atmosphere (99.999%). The heating rate was 10 K min^{-1} and the flow rate of nitrogen was 30 cm^3 min^{-1}. The mass of the sample was 7.9 mg. Two Al_2O_3 crucibles were used (capacity: 100 μL). The reference crucible was filled with α-Al_2O_3. The TG equipment was calibrated by the $CaC_2O_4 \cdot H_2O$ (99.9%).

Results and discussion

Heat capacity

The low-temperature experimental molar heat capacities of the solid compound are shown in Fig. 1 and tabulated in Table 1. The molar heat capacities of the sample are fitted to the following polynomial

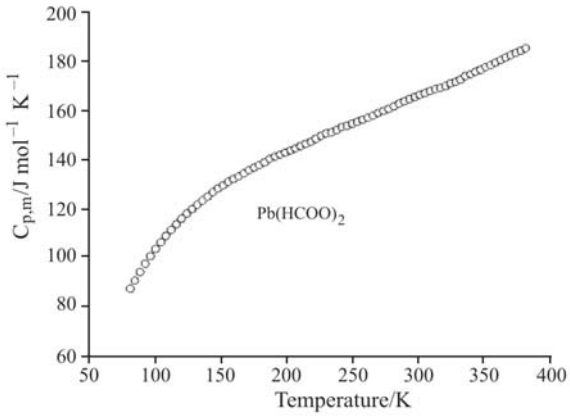

Fig. 1 Experimental molar heat capacities ($C_{p,m}$) of lead formate as a function of the temperature (K)

Table 1 The experimental molar heat capacities of lead formate (molecular formula: $Pb(HCOO)_2$, molar mass: 297.24 g mol^{-1})

Temperature/K	$C_{p,m}$/J mol^{-1} K^{-1}	Temperature/K	$C_{p,m}$/J mol^{-1} K^{-1}	Temperature/K	$C_{p,m}$/J mol^{-1} K^{-1}
80.87	87.326	183.26	138.825	285.70	162.748
84.38	90.585	187.16	140.340	289.68	163.689
88.30	94.110	191.12	141.212	293.62	164.638
92.28	97.518	195.08	142.047	297.55	165.497
96.22	100.598	199.02	142.813	301.46	166.333
100.13	103.500	202.92	143.663	305.36	166.939
104.12	106.272	206.79	144.586	309.29	167.868
108.10	108.843	210.64	145.414	313.26	168.586
112.06	111.292	214.52	146.367	317.21	169.164
116.02	113.579	218.45	147.233	321.12	169.865
119.98	115.833	222.35	148.432	324.98	170.991
123.95	117.956	226.23	149.632	328.76	171.722
127.92	119.804	230.09	150.636	332.49	172.525
131.91	121.547	234.08	151.038	336.29	173.985
135.83	123.233	238.10	152.060	340.12	174.734
139.76	124.873	242.05	153.192	343.99	175.740
143.72	126.641	245.99	153.667	347.84	176.450
147.69	128.190	249.94	154.519	351.69	177.684
151.69	129.479	253.87	155.355	355.51	178.428
155.63	130.839	257.85	156.181	359.31	179.473
159.54	132.045	261.86	157.001	363.09	180.523
163.47	133.135	265.86	157.952	366.91	181.554
167.44	134.307	269.83	158.922	370.77	182.465
171.36	135.609	273.79	159.730	374.60	183.328
175.32	136.686	277.72	160.568	378.42	184.288
179.31	137.686	281.69	161.649	382.22	185.254

equation of heat capacities ($C_{p,m}$) with reduced temperature (X) by means of the least square fitting:

From T=(80 to 380) K

$$C_{p,m}\ [J\ mol^{-1}\ K^{-1}]=150.1516+33.9162X-3.5641X^2+7.2381X^3-9.4935X^4+8.0777X^5-1.4893X^6 \quad (1)$$

where X=(T–230)/150, and T is the experimental temperature, 230 is obtained from polynomial (T_{max}+T_{min})/2, 150 is obtained from polynomial (T_{max}–T_{min})/2, T_{max} is the upper limit (380 K) of the above temperature region, T_{min} is the lower limit (80 K) of the above temperature region. The correlation coefficient of the fitting, R^2=0.9999. Based on Eq. (1), the heat capacity of the sample at 298.15 K was calculated to be 165.243 J mol^{-1} K^{-1}.

From Fig. 1, it can be seen that the heat capacity of the sample increases with increasing temperature in a smooth and continuous manner in the temperature range from 80 to 380 K. In this temperature range, no phase transition or thermal anomaly was observed, which indicates that this sample is stable in the above temperature range.

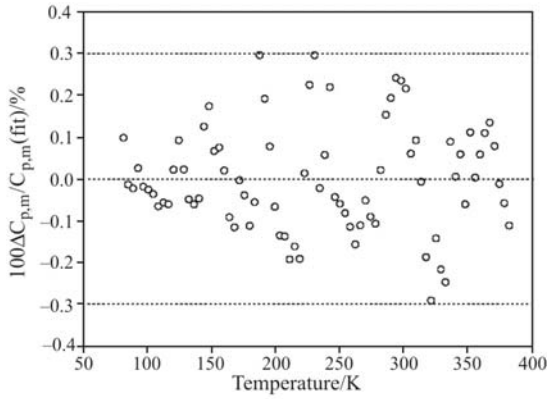

Fig. 2 The plot of relative deviations of the experimental heat capacity values [$C_{p,m}$(exp)] from the fitting heat capacity values [$C_{p,m}$(fit)] *vs*. the absolute temperature (T). $\Delta C_{p,m}$=[$C_{p,m}$(exp)–$C_{p,m}$(fit)]

Figure 2 gives the plot of relative deviations of the experimental heat capacity values of the sample, $C_{p,m}$(exp), from the fitting heat capacity values,

$C_{p,m}$(fit), *vs*. the absolute temperature (T). It can be seen from Fig. 2 that relative deviations of all the experimental points from the fitting heat capacity values are within ±0.30%.

Thermodynamic functions of lead formate

Enthalpy and entropy of substances are basic thermodynamic functions. Through the polynomial representing heat capacity and the relationship between thermodynamic functions and heat capacity, the thermodynamic functions relative to the reference temperature of 298.15 K were calculated in the temperature ranges from 80 to 380 K with an interval of 5 K. The thermodynamic relationships are as follows:

$$H_T - H_{298.15} = \int_{298.15}^{T} C_{p,m}\,dT \quad (2)$$

$$S_T - S_{298.15} = \int_{298.15}^{T} \frac{C_{p,m}}{T}\,dT \quad (3)$$

The values of thermodynamic function H_T–$H_{298.15}$, S_T–$S_{298.15}$ are listed in Table 2.

DSC and TG results

The DSC curve of lead formate in Fig. 3 exhibited four sharp endothermic peaks in the temperature range from 500 to 635 K. Based on the DSC curve, there was no phase transition or other thermal event which was observed below 500 K. Above 500 K, the first significant sharp endothermic peak started at 500 K and ended at 543 K with the peak temperature at 539.0 K. Next to the first peak, immediately, the second peak temperature was 551.9 K and the third peak temperature was 556.9 K. Since two intense endothermic de-

Table 2 Calculated thermodynamic function data of lead formate

T/K	$C_{p,m}$/ J mol^{-1} K^{-1}	H_T–$H_{298.15}$/ kJ mol^{-1}	S_T–$S_{298.15}$/ J mol^{-1} K^{-1}	T/K	$C_{p,m}$/ J mol^{-1} K^{-1}	H_T–$H_{298.15}$/ kJ mol^{-1}	S_T–$S_{298.15}$/ J mol^{-1} K^{-1}
80	86.373	–29.760	–169.04	235	151.278	–9.995	–37.61
85	91.174	–29.316	–163.65	240	152.399	–9.236	–34.41
90	95.597	–28.849	–158.31	245	153.514	–8.471	–31.26
95	99.674	–28.360	–153.04	250	154.625	–7.701	–28.15
100	103.432	–27.852	–147.83	255	155.732	–6.925	–25.08
105	106.901	–27.326	–142.70	260	156.837	–6.144	–22.04
110	110.106	–26.784	–137.66	265	157.940	–5.357	–19.05
115	113.071	–26.226	–132.70	270	159.042	–4.564	–16.09
120	115.818	–25.653	–127.82	275	160.143	–3.766	–13.16
125	118.369	–25.068	–123.04	280	161.243	–2.963	–10.26
130	120.742	–24.470	–118.35	285	162.343	–2.154	–7.40
135	122.956	–23.861	–113.75	290	163.445	–1.339	–4.56
140	125.027	–23.241	–109.24	295	164.547	–0.519	–1.75
145	126.971	–22.611	–104.82	298.15	165.243	0.000	0.00
150	128.800	–21.971	–100.48	300	165.652	0.306	1.02
155	130.529	–21.323	–96.23	305	166.759	1.137	3.78
160	132.168	–20.666	–92.06	310	167.871	1.974	6.50
165	133.728	–20.001	–87.97	315	168.987	2.816	9.20
170	135.220	–19.329	–83.96	320	170.110	3.664	11.86
175	136.651	–18.649	–80.02	325	171.241	4.517	14.50
180	138.030	–17.962	–76.15	330	172.381	5.376	17.10
185	139.363	–17.269	–72.35	335	173.532	6.241	19.66
190	140.657	–16.569	–68.62	340	174.697	7.111	22.18
195	141.918	–15.862	–64.95	345	175.878	7.988	24.65
200	143.150	–15.150	–61.34	350	177.077	8.870	27.07
205	144.358	–14.431	–57.79	355	178.298	9.759	29.41
210	145.546	–13.706	–54.29	360	179.543	10.653	31.68
215	146.716	–12.976	–50.86	365	180.815	11.554	33.86
220	147.872	–12.239	–47.47	370	182.119	12.461	35.93
225	149.017	–11.497	–44.13	375	183.458	13.375	37.87
230	150.152	–10.749	–40.85	380	184.837	14.296	39.66

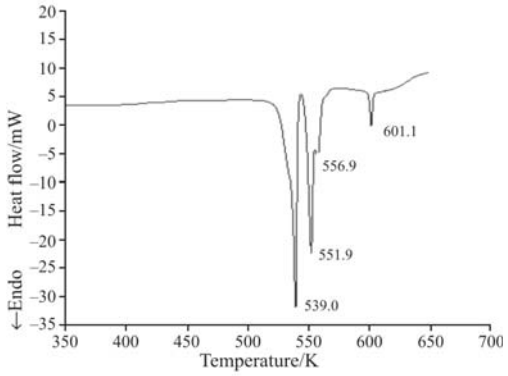

Fig. 3 DSC curve of lead formate under high purity nitrogen atmosphere

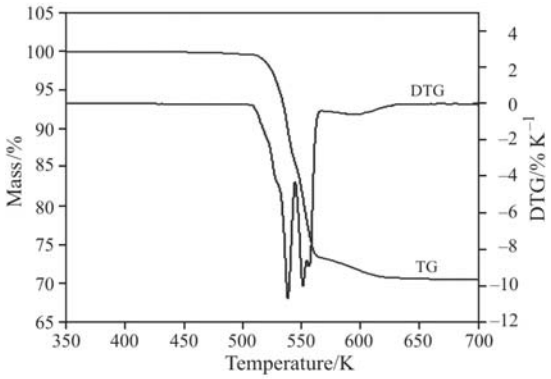

Fig. 4 TG-DTG curves of lead formate under high purity nitrogen atmosphere

composition processes occurred successively, one decomposition process did not finish, and another occurred. The endothermic peak could not be separated, which formed a wide exothermic peak. Between 595 and 635 K range, the fourth peak was observed with the peak temperature at 601.1 K.

From the TG-DTG curve (Fig. 4), TG analysis of lead formate showed that the four-step mass loss occurred in the 500 to 635 K temperature range. The decomposition taking place during heating can be traced as follows:

$$Pb(HCOO)_2 \xrightarrow{10.1\%\ (calcd.),\ 11.0\%\ (exp);\ 500–540\ K} PbCO_3$$

$$PbCO_3 \xrightarrow{9.9\%\ (calcd.),\ 8.8\%\ (exp);\ 540–552\ K} PbCO_3{\cdot}2PbO$$

$$PbCO_3{\cdot}2PbO \xrightarrow{7.6\%\ (calcd.),\ 6.9\%\ (exp);\ 552–565\ K} PbO{\cdot}Pb$$

$$PbO{\cdot}Pb \xrightarrow{2.7\%\ (calcd.),\ 2.9\%\ (exp);\ 565–635\ K} Pb$$

The first mass loss was about 11.0% likely due to the decomposition from lead formate to lead carbonate, which roughly coincides with the calculated value of 10.1% in the 500–540 K range. Further decomposition of lead carbonate occurred in the region of 540–552 K and the mass loss was 8.8%, which was probably decomposed to the complex of lead carbonate and lead monoxide ($PbCO_3{\cdot}2PbO$). These two steps were in agreement with that reported in literature [5]. Subsequently, the third rapid loss of 6.9% and the fourth slow loss of 2.9% were observed above 552 K, and there was some complex of lead monoxide and lead ($PbO{\cdot}Pb$) between the two processes. The overall mass loss of the sample was ca. 29.6% in accord with the calculated percentage (30.3%). Furthermore, the brown residue was found in the crucible after the experiment was completed. We considered that the brown residue should be the metal with a little amount of lead monoxide under nitrogen atmosphere.

The further investigation of hydrogen storage performance for the compound is in process of study in our laboratory.

Acknowledgements

The authors gratefully acknowledge the National Nature Science Foundation of China for financial support to this work under Grant No. 20473091.

References

1 J. L.C. Rowsell and O. M. Yaghi, Micropor. Mesopor. Mater., 73 (2004) 3.
2 S. Kitagawa, R. Kitaura and S. Noro, Angew. Chem. Int. Ed., 43 (2004) 2334.
3 P. G. Harrison and A. T. Steel, J. Organomet. Chem., 239 (1982) 105.
4 R. C. Weast, CRC Handbook of Chemistry and Physics, 62nd Ed. (Chemical Rubber, Boca Raton, FL 1981).
5 K. Betzler, H. Hesse, R. Jaquet and D. Lammers, J. Appl. Phys., 87 (2000) 2.
6 P. Baraldi, Spectrochim. Acta A, 37 (1981) 99.
7 M. N. Ray and N. D. Sinnarkar, J. Inorg. Nucl. Chem., 35 (1973) 1373.
8 V. G. Bessergenev, Y. A. Kovalevskaya, L. G. Lavrenova and I. E. Paukov, J. Therm. Anal. Cal., 75 (2004) 331.
9 J. Boerio-Goates, R. Stevens, B. Lang and B. F. Woodfield, J. Therm. Anal. Cal., 69 (2002) 773.
10 V. A. Drebushchak, E. V. Boldyreva, Y. A. Kovalevskaya, I. E. Paukov and T. N. Drebushchak, J. Therm. Anal. Cal., 79 (2005) 65.
11 V. Rohac, M. Fulem, H. G. Schmidt, V. Ruzicka, K. Ruzicka and G. Wolf, J. Therm. Anal. Cal., 70 (2002) 455.
12 L. Wang, Z. C. Tan, S. H. Meng, D. B. Liang, S. T. Ji and Z. K. Hei, J. Therm. Anal. Cal., 66 (2001) 409.
13 Z. C. Tan, B. Xue, S.W. Lu, S. H. Meng, X. H. Yuan and Y. S. Song, J. Therm. Anal. Cal., 63 (2000) 297.
14 D. A. Ditmars, S. Ishihara, S. S. Chang, G. Bernstein and B. D. West, J. Res. Natl. Bur. Stand., 87 (1982) 159.

Received: January 16, 2006
Accepted: January 31, 2006
OnlineFirst: May 23, 2006

DOI: 10.1007/s10973-006-7510-9